Exchange Interaction in an InSb Quantum Well Measured with Landau-Level Tunneling Spectroscopy

S. K. Clowes,[1] C. P. Allford,[2] D. Shearer,[1] G. V. Smith,[2] R. Simmons,[1]
B. N. Murdin,[1] U. Zeitler,[3,4] and P. D. Buckle[2]
[1]*Advanced Technology Institute, University of Surrey, Guildford GU2 7XH, United Kingdom*
[2]*School of Physics and Astronomy, Cardiff University, Queen's Buildings, Cardiff CF24 3AA, United Kingdom*
[3]*High Field Magnet Laboratory (HFML-EMFL), Radboud University, Toernooiveld 7, 6525 ED Nijmegen, The Netherlands*
[4]*Institute for Molecules and Materials, Radboud University, Heyendaalseweg 135, 6525 AJ Nijmegen, The Netherlands*

(Received 4 June 2025; accepted 22 August 2025; published 29 September 2025)

We studied InSb quantum well devices using Landau-level tunneling spectroscopy through a three-terminal differential conductance technique. This method is similar to filled-state scanning tunneling microscopy but uses a stationary contact instead of a mobile tip to analyze the two-dimensional electron system. Applying magnetic fields up to 15 T, we identified clear peaks in the differential current-voltage profiles, indicative of Landau-level formation. By examining deviations from the expected Landau fan diagram, we extract an absolute value for the exchange-induced energy shift. Through an empirical analysis, we derive a formula describing the exchange shift as a function of both magnetic field strength and electron filling. Our findings indicate that the emptying of the $\nu = 2$ and $\nu = 3$ Landau levels causes an exchange interaction energy shift in the $\nu = 1$ level. Unlike prior studies that infer level energies relative to one another and report oscillatory g-factor behavior, our method references the energy of the Landau levels above the filled states of the contact under a bias voltage, revealing that only the ground state Landau level experiences a measurable exchange shift.

DOI: 10.1103/rr3f-3zhd

Introduction—The exploration of quantum behavior in two-dimensional semiconductors subjected to strong magnetic fields has been a prominent research focus since the identification of the quantum Hall effect [1]. Among these studies, the spectroscopic analysis of Landau levels has generated significant interest, particularly the exchange enhancement phenomenon [2–4]. In such systems, the electron energy is characterized by a combination of kinetic energy and exchange energy, the latter originating from the exchange interactions between electrons across different Landau levels.

The enhancement of the effective g factor as a function of the external magnetic field has been widely reported and is commonly attributed to the exchange interaction between electrons [2,3,5–17]. This phenomenon was first investigated by Fang and Stiles in 1968 [18], who observed a variation in the g factor with surface electron concentration in Si inversion layers under tilted magnetic fields. This tilted field enhances Zeeman splitting while preserving Landau quantization, which depends only on the perpendicular field component. The enhancement of the g factor is quantified by identifying the field orientation in which adjacent Landau levels align. This method has since been widely adopted in the study of low-dimensional systems and for the understanding of many-body effects in quantum wells.

This enhancement in the exchange interaction is commonly linked to the polarization of electron spin of the spin-split Landau levels. Based on the findings of Fang and Stiles [18], Ando and Uemura [4] predicted an oscillation in the g factor originating from the electron spin polarization when the Landau levels intersect the Fermi energy. The nature of g-factor measurements is that they are relative measurements of energy splitting between two Landau levels, either using the tilted-field coincidence [7,16,18–23] or optical spectroscopic measurements [24,25]. Reports of oscillating g factors in III–V semiconductors [13,26,27] stem partly from flawed Shubnikov–de Haas analysis methods [28,29] that misattribute periodicity shifts to g^* variations.

In this Letter, we report on three-terminal differential conductance measurements, which enables a direct measurement of Landau levels and the exchange enhancement effect. This method is similar to an earlier report of Landau-level spectroscopy of a GaAs surface two-dimensional system, using tunneling through an InAs/AlAs quantum dot [3]. However, this study has been carried out in a δ-doped quantum well system where tunneling is through a delta-doped layer rather than a single zero-dimensional ground state in a quantum dot. Another distinction lies in the study of an InSb/AlInSb quantum well (QW), where the InSb 2D system exhibits the largest bulk g^* and the smallest effective mass (m^*) among the III–V binary compounds. These material properties lead to a rapid separation of the Landau levels into clearly identifiable Zeeman split-spin states at comparatively low magnetic fields, thereby allowing a clear and absolute measurement of the exchange interaction in this system.

Experimental methods—Experiments were performed on material grown by solid source molecular beam epitaxy on semi-insulating, lattice-mismatched GaAs substrates. In growth order, the epitaxy comprises an aluminium antimonide (AlSb) accommodation layer, a 3 μm $Al_{0.1}In_{0.9}Sb$ strain-relieving barrier layer (to allow for lattice mismatch relaxation), a 30 nm InSb quantum well layer, and a 50 nm $Al_{0.15}In_{0.85}Sb$ top barrier layer. Tellurium δ doping is introduced only into the top barrier, 25 nm above the InSb quantum well. Deliberate doping of the lower barrier is avoided in order to prevent any impurity donor atoms from being carried forward on the growth plane, which could significantly compromise the transport lifetime of carriers in the quantum well. The quantum wells have been modeled using the Schrödinger-Poisson software Nextnano [30], shown in Fig. 1, to determine subband states confined within the QW. The Γ point of the first subband E_1 is located 43 meV below the Fermi energy $E_F = 0$, and indicates occupation of the second subband and states within the δ-doped region. The energy of the conduction band at the surface is set to be $1/3(\approx 0.17\ \mathrm{eV})$ of the $Al_{0.15}In_{0.85}Sb$ band gap (≈ 0.51 eV) above E_F. Note that this Schrödinger-Poisson model excludes the effects from the diffusion of Zn under the metal contact.

Devices were fabricated using standard photolithography techniques into six contact hall bars with a nominal distance of 200 μm between longitudinal contacts and 40 μm between transverse contacts. To form ohmic contacts, a Zn keying layer (around 10 nm) is initially deposited to improve adhesion to the surface followed by a thick Au layer (300 nm). These are evaporated while the substrate is heated to 100 °C to promote diffusion of the metal ions on the surface and minimize Schottky contact formation. Shubnikov–de Haas measurements were performed to determine the low-temperature carrier concentration $n = 3.14 \times 10^{15}\ \mathrm{m}^{-2}$, and to estimate the broadening of the Landau levels and the $|g^*|$; see Supplemental Material (SM) [31]. In this investigation, a three-terminal differential conductance measurement was carried out on an InSb/InAlSb heterostructure; see Fig. 2(a). The three-terminal geometry isolates tunneling between the 2DEG and the contact by localizing the voltage drop at the common contact. A further explanation of this geometry is provided in SM. Using a force bias voltage with a 3 mV modulation, a software lock-in method was used to simultaneously record both the three-terminal differential conductance and I–V measurements of the InSb/InAlSb QW devices in a liquid helium bath at 4 K in fields up to 15 T.

Results—A typical I–V and differential conductance plots are shown in Fig. 2 for forward bias in a magnetic field of 3.5 T. The I–V characteristics exhibit a stepwise increase in current with increasing bias voltage, which

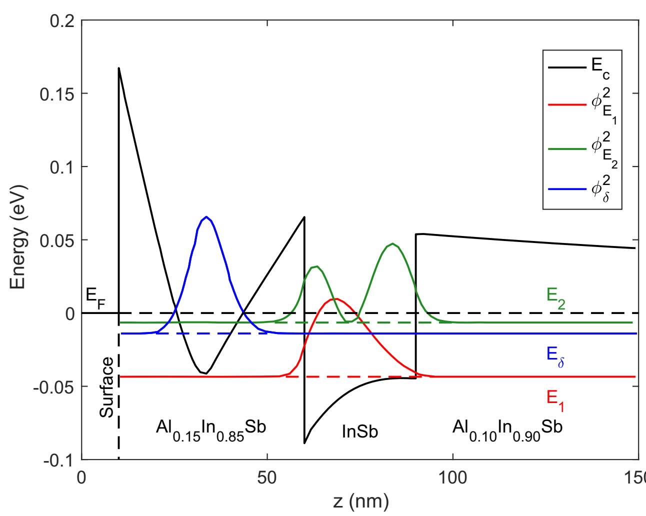

FIG. 1. The zero bias band structure and wave function solutions of the InSb/InAlSb QW, calculated using Nextnano's Schrödinger-Poisson solver. The Fermi energy $E_F = 0$.

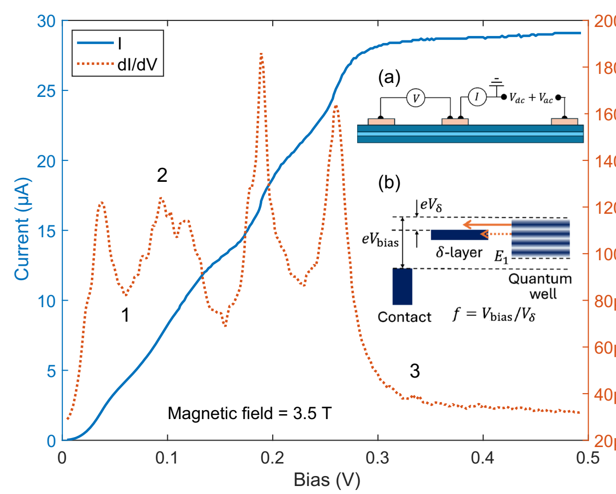

FIG. 2. A typical three-terminal conductance measurement at 3.5 T, with peak-to-peak ac voltage $V_{ac} = 2$ mV at 33 Hz. The solid line shows the I–V measurement that aligns with the peaks seen in the dI/dV dotted line. (1) Minima in dI/dV, corresponding to filled upper states of the δ layer aligned between Landau levels. (2) Peak in dI/dV, corresponding to an increase in tunneling as a Landau level passes through the filled upper states of the δ layer and can tunnel into empty states. (3) Saturation, corresponding to the state where all Landau levels can tunnel into empty states. (a) Inset shows circuit diagram of three-terminal measurement. (b) Schematic of tunneling from Landau levels in quantum well through δ-layer subband into metal contact under bias. The condition shown corresponds to the minima (1) in dI/dV at which the upper filled states in the δ layer lies between the $\nu = 3$ and four Landau levels, such that tunneling from the $\nu = 3$ level is blocked.

saturates at approximately 0.3 V with a current of 28 μA. These steps are manifested as peaks in the differential conductance. This is analogous to filled-state scanning tunneling microscopy (STM), where filled states tunnel into empty states in the tip [35]. A study using this STM technique has reported Landau-level spectroscopy of a Cs-induced inversion layer on the surface of InSb [36], in which a small oscillation was observed in the exchange interaction for high filling factors. In this study, the filled states in the QW tunnel into empty states above the Fermi energy (E_F) in the metal contact. In the example shown in Fig. 2 at 3.5 Tesla, there are four filled Landau levels below E_F. As the bias voltage is increased the upper filled Landau level is raised above the Fermi level of the metal contact (region 1), allowing electrons to tunnel into the empty states and giving rise to a step increase in the current and the first peak in the differential conductance. Increasing the bias further brings more Landau levels above the Fermi level of the metal contact, where peaks in the differential conductance correspond to the condition where the Landau level passes through the Fermi level of the metal contact (region 2), allowing the electrons to tunnel into empty states. Eventually, all of the Landau levels, i.e., all the filled states in the QW, are raised above the Fermi level of the metal contact such that the current saturates (region 3).

A differential conductance intensity plot as a function of applied magnetic field and bias voltage is shown in Fig. 3, which exhibits a Landau-level fan with the first four spin-split levels labeled with filling factor ν (raw data available at Ref. [37]). The additional texture in the Landau fan plot is due to the density of states of the contact, since the tunneling current is a product of the density of states of the quantum well and the contact. At higher magnetic fields above 5 T, oscillations in differential conductance that have the opposite field dependence to the Landau levels are observed. These features can be explained by the formation of Landau levels in the δ layer. Above 4 T, the $\nu = 1$ Landau level shows a noticeable downward shift due to exchange, labeled E_{ex}, which we quantify by fitting the Landau fan. To model the Landau fan plot, which includes the spin-orbit interaction, we adopt the formalism of Bychkov and Rashba [38,39] such that

$$E = E_{l,\lambda} = \hbar\omega_c\left[l - \frac{\lambda}{2}\sqrt{(1-Z)^2 + lS^2}\right], \qquad (1)$$

where $l = 0, 1, 2, \ldots$ is a positive integer, $\lambda = \pm 1$ ($\lambda = +1$ only for $l = 0$) and $\omega_c = eB/m^*(E)$ is the cyclotron frequency, B is the perpendicular applied magnetic field, and $m^*(E)$ is the effective mass that includes the effects of nonparabolicity as the band energy dispersion of InSb is highly nonparabolic due to its small band gap. The Rashba spin orbit and Zeeman terms are given by

$$S = \frac{\alpha\sqrt{2}}{\hbar\omega_c l_B}, \qquad Z = \frac{g^*(E)m^*(E)}{2m_0}, \qquad (2)$$

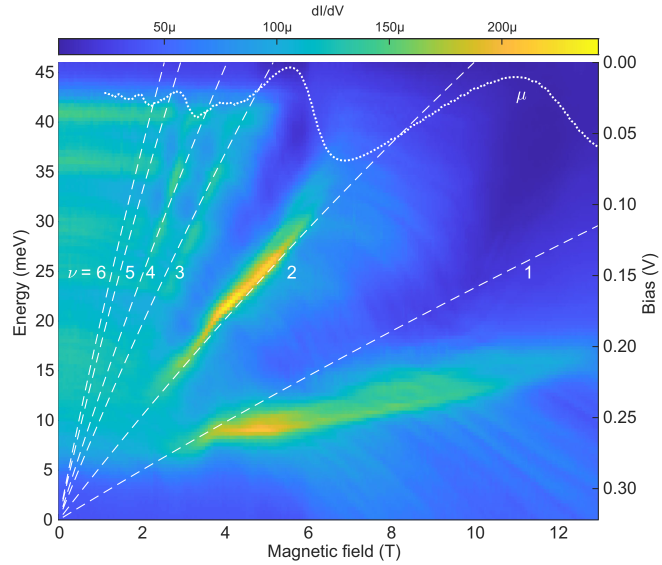

FIG. 3. Differential conductance as a function of bias and magnetic field. The calculated energies of Landau-level fan plot overlaid on the differential conductance data, as determined through fitting to the extracted peaks in the differential conductance for the first four Landau levels: $\nu = 1(l = 0, \lambda = +1)$, $\nu = 2(l = 1, \lambda = -1)$, $\nu = 3(l = 1, \lambda = +1)$, $\nu = 4(l = 2, \lambda = -1)$, $\nu = 5(l = 2, \lambda = +1)$, and $\nu = 6(l = 3, \lambda = -1)$. The bias is converted to Landau-level energy using fitting parameters E_1 and f. The calculated electrochemical potential μ is also shown; see SM.

where α is the Rashba parameter, $l_B = \sqrt{\hbar/eB}$ is the magnetic length, m_0 is the free electron mass, and $g^*(E)$ is the g factor, which also includes the effects of nonparabolicity. We obtain the theoretical estimates of both the effective mass $m^*(\Gamma) = 0.013m_0$ and g factor $g^*(\Gamma) = -47$ at the Γ point from $\mathbf{k}\cdot\mathbf{p}$ theory; see SM. To incorporate the nonparabolicity into the Landau fan plot calculation, an approximation in the limit where $m^*(\Gamma) \ll 1$ and $g^*(\Gamma) \gg 2$ is used, such that

$$m^*(E) \approx m^*(\Gamma)(1 + \Lambda E), \qquad (3)$$

$$g^*(E) \approx \frac{g^*(\Gamma)}{1 + \Lambda E}, \qquad (4)$$

where $\Lambda \approx 1/(E_0 + E_c) = 4.0\ \mathrm{eV}^{-1}$.

We see that the Zeeman term Z is unaffected by nonparabolicity due to the product $m^* g^*$ being independent of Λ. The Rashba term S is also is unaffected by nonparabolicity as both ω_c and the Rashba parameter α scale inversely with m^* [40]. The Landau energies including nonparabolicity are therefore

$$\Lambda E^2 + E - \frac{\hbar e B}{m^*(\Gamma)}\left[l - \frac{\lambda}{2}\sqrt{(1-Z)^2 + lS^2}\right] = 0. \qquad (5)$$

TABLE I. Comparison of parameters obtained from theoretical values or through modeling with those obtained from the experimental fits to the Landau fan accounting for nonparabolicity $\Lambda = 4.0\ \mathrm{eV}^{-1}$.

Parameter	Theoretical/modeled	Experimental fit
$m^*(\Gamma)$	$0.0131m_0$	$0.0145m_0$
$\lvert g^*(\Gamma)\rvert$	47	50
E_1	−43 meV	−46 meV
Leverage factor f	–	7.0 V/eV

The Landau-level energies can be extracted by taking the positive solutions to this quadratic equation. To fit a Landau fan to the data, there are now four material-specific fitting parameters: $m^*(\Gamma)$, $|g^*(\Gamma)|$, Λ, and α. To reduce the number of free fitting parameters the values of $\Lambda = 4.0\ \mathrm{eV}^{-1}$ and $\alpha = 0.1$ eV Å [41] were fixed. The latter has minimal effect on the Landau fan plot at the fields used in this study.

Robust fitting was found with $|g^*(\Gamma)| = 50$, $m^*(\Gamma) = 0.0145m_0$, $E_1 = -47$ meV using a leverage factor $f = 7.0$ V/eV, which is defined as the bias voltage required to produce a relative energy shift of E_1 with respect to the upper filled state in the δ layer; see Fig. 2 inset (b). See SM for more details of the fitting process. The value of $m^*(\Gamma)$ is higher than predicted from $\mathbf{k}\cdot\mathbf{p}$ theory, although it is within the experimentally measured range. The agreement of the fitting parameters with those predicted from theory (see Table I for summary) provides confidence in the value of the obtained leverage factor, which ultimately determines the magnitude of the observed shift in energy of the first Landau level above 4 T. We discount the possibility of a field dependence on the leverage factor as the fit to the Landau fan plot for $\nu = 2$ maintains good accuracy well beyond 4 T, past the stage at which the shift in the $\nu = 1$ level becomes evident.

The measured shift in energy E_{ex} of the $\nu = 1$ level is shown in Fig. 4 as a function of the magnetic field. This was calculated by taking the difference between the sampled peak values in the measured data from the expected Landau-level energy using the best-fit parameters in Table I. In a magnetic field of 11 T the observed shift is approximately 11 meV, at a field where the majority of electrons occupy the ground state Landau level. The relationship between this exchange energy shift and the electron occupation of Landau levels will be discussed in the next section.

Discussion—Previously, the shift in energy due to the exchange enhancement is assumed to be proportional to the polarization of the ground state Landau level [2]. We adopt a more nuanced approach, taking into account the exchange interaction between electrons in the ground state Landau level ($\nu = 1$) and Landau levels with higher filling factors ($\nu > 1$). In order to investigate this, the following equation was used to define the strength of E_{ex}:

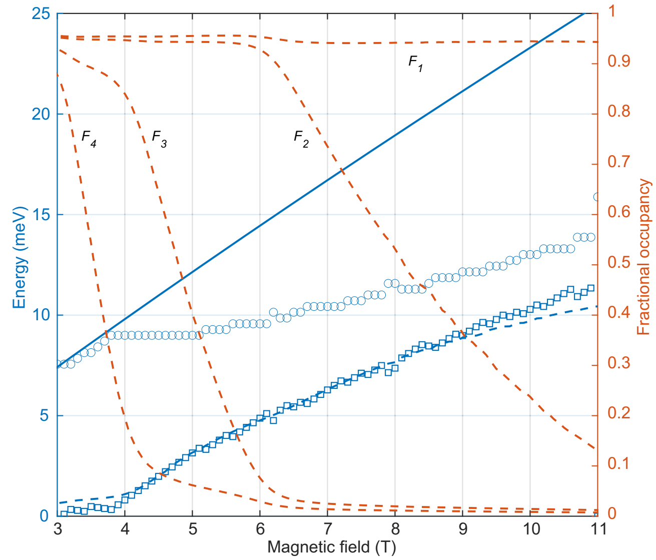

FIG. 4. The energy and exchange energy shift for the ground state ν_1 Landau level. Solid line: calculated Landau-level energy for $\nu = 1$. Circles: measured $\nu = 1$, squares measured E_{ex}. Dotted line: fit to E_{ex} using Eq. (6). Also shown are the calculated fractional electron occupation of the first four Landau Levels plotted as a function of the magnetic field at 4 K.

$$E_{\mathrm{ex}} = \sum_{\nu=2} E_{\mathrm{ex}}^{\nu}(1 - F_\nu), \tag{6}$$

where E_{ex}^{ν} are coefficients representing the product of the Coulomb interaction and the exchange integral between the ground state Landau level and the Landau level with filling factor ν, and F_ν is the fractional electron occupation of the higher Landau level.

The fractional occupations were determined by numerically solving the broadened Landau-level density of states at finite temperature (details in SM). Plotting these electron occupations shows that the $\nu = 4$ level starts to deplete at approximately 3 T before any detectable shift in the $\nu = 1$ level occurs; see Fig. 4. Notably, this shift aligns with the onset of the depletion for the $\nu = 3$ level at around 4 T.

The expression in Eq. (6) is fitted using a linear regression to obtain the coefficients of $E_{\mathrm{ex}}^2 = 6.6$ meV and $E_{\mathrm{ex}}^3 = 4.6$ meV, with negligible values for E_{ex}^4 and above, with the fit obtained shown in Fig. 4. This empirical, phenomenological method of investigating the behavior of electrons in a 2DEG quantum well provides evidence that the $\nu = 2$ and $\nu = 3$ levels have similar interaction strengths with the $\nu = 1$ level. The slight deviation between the measured exchange shift and the fit of E_{ex} could be attributed to a further reduction in the coulomb interaction between electrons in the $\nu = 1$ level as they become more localized due to the reduction of the magnetic length, which is proportional to $1/\sqrt{B}$.

Conclusions—We have presented an absolute measurement of the Landau fan in InSb quantum wells using a three-terminal differential conductance technique. This method enables direct investigation of the electronic behavior in the presence of large external magnetic fields. Unlike conventional approaches that determine Landau-level energies relative to other field-dependent levels, our technique leverages a relative linear shift in the states in the Landau levels with the upper filled states in the δ-layer barrier. This allows for the measurement of the level energies independently of other levels. Our results reveal a distinct deviation of the ground state $\nu = 1$ Landau level from the expected fan diagram, a deviation attributed to the exchange interaction. Interestingly, this spectroscopic technique does not indicate similar deviations for higher Landau levels ($\nu > 1$), contradicting previous reports of oscillatory behavior in the effective g factor. A potential explanation for this observation is rooted in the spatial distribution and spin configuration of the Landau-level wave functions. At high fields, the reduced cyclotron radius promotes spin polarization and spatial separation, suppressing Coulomb repulsion in the $\nu = 1$ level. This limits the self-exchange energy in the ground state. As the magnetic field decreases and higher Landau levels become occupied, strong exchange interactions arise between the $\nu = 1$ level and partially filled levels of the same spin. In particular, the $\nu = 3$ level, which shares the same spin orientation as $\nu = 1$, couples strongly via exchange. As $\nu = 3$ depopulates, this strong coupling enables electrons in both levels to reconfigure, thereby reducing their mutual Coulomb interaction and leading to a measurable shift in the energy of the ground state. The $\nu = 2$ level, although of opposite spin, also contributes to the exchange shift via Coulomb interaction, and its depletion similarly reduces the interaction strength. In contrast, levels such as $\nu = 4$ are either spin-paired or more weakly interacting due to reduced overlap or screening, and thus have negligible influence. These effects explain why only the $\nu = 2$ and $\nu = 3$ levels significantly affect the exchange shift of the $\nu = 1$ Landau level.

In summary, these findings highlight that the exchange interaction selectively affects the ground state spin-split Landau level and does not manifest as a global modification of the g factor. Thus, describing the exchange shift as a renormalized g factor is misleading; the interaction is independent of spin magnetic moment and better treated as a distinct exchange effect.

Acknowledgments—This work was supported by HFML-RU/NWO-I, a member of the European Magnetic Field Laboratory (EMFL). The authors gratefully acknowledge EPSRC (UK) for Grant No. EP/L012995/1 and for a studentships for D. S., G. V. S. and R. S.

Data availability—The data that support the findings of this Letter are openly available [37].

[1] K. v. Klitzing, G. Dorda, and M. Pepper, New method for high-accuracy determination of the fine-structure constant m, based on quantized Hall resistance, Phys. Rev. Lett. **45**, 494 (1980).

[2] R. J. Nicholas, R. J. Haug, K. V. Klitzing, and G. Weimann, Exchange enhancement of the spin splitting in a GaAs-GaxAl1-xAs heterojunction, Phys. Rev. B **37**, 1294 (1988).

[3] P. C. Main, A. Thornton, R. J. A. Hill, S. T. Stoddart, T. Ihn, L. Eaves, K. A. Benedict, and M. Henini, Landau-level spectroscopy of a two-dimensional electron system by tunneling through a quantum dot, Phys. Rev. Lett. **84**, 729 (2000).

[4] Tsuneya Ando and Yasutada Uemura, Oscillation of effective g factor in MOS inversion layers under strong magnetic fields, Jpn. J. Appl. Phys. **13**, 329 (1974).

[5] Ryuichi Masutomi and Tohru Okamoto, Adsorbate-induced quantum Hall system probed by scanning tunneling spectroscopy combined with transport measurements, Appl. Phys. Lett. **106**, 251602 (2015).

[6] Xiaoyang Mu, Gerard Sullivan, and Rui-Rui Du, Effective g-factors of carriers in inverted InAs/GaSb bilayers, Appl. Phys. Lett. **108**, 012101 (2016).

[7] Ning Tang, Kui Han, Fang-Chao Lu, Jun-Xi Duan, Fu-Jun Xu, and Bo Shen, Exchange enhancement of spin-splitting in AlxGa1-xN/GaN heterostructures in tilted magnetic fields, Chin. Phys. Lett. **28**, 037103 (2011).

[8] L. S. Bovkun, S. S. Krishtopenko, M. S. Zholudev, A. V. Ikonnikov, K. E. Spirin, S. A. Dvoretsky, N. N. Mikhailov, F. Teppe, W. Knap, and V. I. Gavrilenko, Exchange enhancement of the electron g-factor in a two-dimensional semimetal in HgTe quantum wells, Semiconductors **49**, 1627 (2015).

[9] S. S. Krishtopenko, V. I. Gavrilenko, and M. Goiran, Exchange enhancement of g-factor in narrow-gap InAs/AlSb quantum well heterostructures, Solid State Phenom. **190**, 554 (2012).

[10] M. Hayne, A Usher, J. J. Harris, and C. T. Foxon, Exchange enhancement of the Landau-level separation for two-dimensional electrons in GaAs/Ga1-xAlxAs heterojunctions, Phys. Rev. B **46**, 9515 (1992).

[11] S. S. Krishtopenko, K. V. Maremyanin, K. P. Kalinin, K. E. Spirin, V. I. Gavrilenko, N. V. Baidus, and B. N. Zvonkov, Exchange enhancement of the electron g factor in strained InGaAs/InP heterostructures, Semiconductors **49**, 191 (2015).

[12] B. Nedniyom, R. J. Nicholas, M. T. Emeny, L. Buckle, A. M. Gilbertson, P. D. Buckle, and T. Ashley, Giant enhanced g-factors in an InSb two-dimensional gas, Phys. Rev. B **80**, 125328 (2009).

[13] A. Raymond, J. L. Robert, C. Bousquet, W. Zawadzki, F. Alexandre, and I. M. Masson, Gigantic exchange enhancement of spin g-factor for two-dimensional electron gas in GaAs, Solid State Commun. **55**, 271 (1985).

[14] S. S. Krishtopenko, K. P. Kalinin, V. I. Gavrilenko, Yu. G. Sadofyev, and M. Goiran, Rashba spin splitting and exchange enhancement of the g factor in InAs/AlSb heterostructures with a two-dimensional electron gas, Semiconductors **46** (2012).

[15] I. G. Savel'ev, A. M. Kreshchuk, S. V. Novikov, A. Y. Shik, G. Remenyi, Gy Kovács, B. Pôdör, and G. Gombos, Spin splitting of the Landau levels and exchange interaction of a non-ideal two-dimensional electron gas in heterostructures, J. Phys. Condens. Matter **8**, 9025 (1996).

[16] R. J. Haug, K. von Klitzing, R. J. Nicholas, J. C. Maan, and G. Weimann, The influence of a tilted magnetic field on the fractional quantum Hall effect and the exchange enhancement of the spin splitting, Surf. Sci. **196** (1988).
[17] S. S. Krishtopenko, V. I. Gavrilenko, and M. Goiran, Theory of g-factor enhancement in narrow-gap quantum well heterostructures, J. Phys. Condens. Matter 23, 385601 (2011).
[18] F. F. Fang and P. J. Stiles, Effects of a tilted magnetic field on a two-dimensional electron gas, Phys. Rev. **174**, 823 (1968).
[19] S. Brosig, K. Ensslin, and A. Jansen, InAs-AlSb quantum wells in tilted magnetic fields, Phys. Rev. B **61**, 13045 (2000).
[20] Sudhakar Yarlagadda, Magnetization instabilities at tilted magnetic fields in the quantum Hall regime, Phys. Rev. B **44**, 13101 (1991).
[21] G. F. Giuliani and J. J. Quinn, Spin-polarization instability in a tilted magnetic field of a two-dimensional electron gas with filled landau levels, Phys. Rev. B **31**, 6228 (1985).
[22] Zijin Lei, Christian A. Lehner, Km Rubi, Erik Cheah, Matija Karalic, Christopher Mittag, Luca Alt, Jan Scharnetzky, Peter Märki, Uli Zeitler, Werner Wegscheider, Thomas Ihn, and Klaus Ensslin, Electronic g factor and magnetotransport in InSb quantum wells, Phys. Rev. Res. **2**, 033213 (2020).
[23] Rayda Gammag and Cristine Villagonzalo, Two-dimensional electron gas tilt-induced Landau level crossings, Solid State Commun. **156**, 16 (2013).
[24] B. B. Goldberg, D. Heiman, and A. Pinczuk, Exchange enhancement of a spin-polarized 2D electron gas determined by optical-absorption spectroscopy, Phys. Rev. Lett. **63**, 1102 (1989).
[25] A. Pinczuk, B. S. Dennis, ' D. Heiman, C. Kallin, L. Brey, C. Tejedor, S. Schmitt-Rink, L. N. Pfeiffer, and K. W. West, Spectroscopic measurement of large exchange enhancement of a spin-polarized 2d electron gas, Phys. Rev. Lett. **68**, 3623 (1992).
[26] Yu G. Sadofyev, A. Ramamoorthy, J. P. Bird, S. R. Johnson, and Y.-H. Zhang, Large g-factor enhancement in high-mobility InSb\AlSb quantum wells, Appl. Phys. Lett. **81**, 1833 (2002).
[27] V. Ya Aleshkin, V. I. Gavrilenko, A. V. Ikonnikov, S. S. Krishtopenko, Yu G. Sadofyev, and K. E. Spirin, Exchange enhancement of the g factor in InAs/AlSb heterostructures, Semiconductors **42**, 828 (2008).
[28] V. I. Nizhankovskii, B. K. Medvedev, and V. G. Mokerov, Chemical-potential and g-factor of a 2d electron-gas in a strong magnetic field, JETP Lett. **47**, 410 (1988), http://jetpletters.ru/ps/0/article_16527.shtml.
[29] V. I. Nizhankovskii, Thermodynamics of two-dimensional electron gas in a magnetic field, Phys. Res. Int. **2011**, 742158 (2011).
[30] Stefan Birner, Tobias Zibold, Till Andlauer, Tillmann Kubis, Matthias Sabathil, Alex Trellakis, and Peter Vogl, Nextnano: General purpose 3-d simulations, IEEE Trans. Electron Devices **54**, 2137 (2007).
[31] See Supplemental Material at http://link.aps.org/supplemental/10.1103/rr3f-3zhd, which includes Refs. [32–34], for details provided for Shubnikov-de Haas Measurements, three terminal measurement, theoretical $\mathbf{k}\cdot\mathbf{p}$ calculations, fitting procedure to Landau fan plot and calculations of fractional occupation of Landau-levels.
[32] Thomas Ihn, *Semiconductor Nanostructures: Quantum States and Electronic Transport* (Oxford University Press, Oxford, 2009).
[33] Claudine Hermann and Claude Weisbuch, $\mathbf{k}\cdot\mathbf{p}$ perturbation theory in III-V compounds and alloys: A reexamination, Phys. Rev. B **15**, 823 (1977).
[34] Roland Winkler, *Spin-orbit Coupling Effects in Two-Dimensional Electron and Hole Systems*, (Springer, Berlin, Heidelberg, 2003).
[35] J. Tersoff and D. R. Hamann, Theory of the scanning tunneling microscope, Phys. Rev. B **31**, 805 (1985).
[36] S. Becker, C. Karrasch, T. Mashoff, M. Pratzer, M. Liebmann, V. Meden, and M. Morgenstern, Probing electron-electron interaction in quantum Hall systems with scanning tunneling spectroscopy Phys. Rev. Lett. **106**, 156805 (2011).
[37] S. K. Clowes, D. Shearer, and Uli Zeitler, Raw Dataset for Exchange interaction in an InSb quantum well measured with Landau-level tunnelling spectroscopy, Zenodo, 10.5281/zenodo.16961716.
[38] Yu A. Bychkov and E. I. Rashba, Oscillatory effects and the magnetic susceptibility of carriers in inversion layers, J. Phys. C **17**, 6039 (1984).
[39] Daniel Hernangómez-Pérez, Jascha Ulrich, Serge Florens, and Thierry Champel, Spectral properties and local density of states of disordered quantum Hall systems with Rashba spin-orbit coupling, Phys. Rev. B **88**, 245433 (2013).
[40] E. A. de Andrada e Silva, G. C. La Rocca, and F. Bassani, Spin-split subbands and magneto-oscillations in iii-v asymmetric heterostructures, Phys. Rev. B **50**, 8523 (1994).
[41] Juerong Li, A. M. Gilbertson, K. L. Litvinenko, L. F. Cohen, and S. K. Clowes, Transverse focusing of spin-polarized photocurrents, Phys. Rev. B **85**, 045431 (2012).